Cardiovascular Reviews, 2025, Volume 3, Issue 4
http://ojs.bbwpublisher.com/index.php/CR
Online ISSN: 2981-8109
Print ISSN: 3083-4880

Prediction of Rapidly Progressing Coronary Plaques Using a 3D Convolutional Neural Network Model Based on Coronary CT Angiography

Wentao Zhang[1], Bingcang Huang[2], Weiping Lu[2], Ying Wang[2], Guangjie Sun[1], Jiahong Xu[3], Zhiru Ge[3]*

[1]School of Gongli Hospital Medical Technology, University of Shanghai for Science and Technology, Shanghai 200093, China
[2]Department of Radiology, Gongli Hospital of Shanghai Pudong New Area, Shanghai 200135, China
[3]Department of Cardiology, Gongli Hospital of Shanghai Pudong New Area, Shanghai 200135, China

**Author to whom correspondence should be addressed.*

Abstract: *Objective*: To develop a three-dimensional convolutional neural network (3D-CNN) model based on coronary computed tomography angiography (CCTA) for predicting rapid plaque progression (RPP), and to compare its performance against traditional machine learning models and existing advanced methodologies. *Methods*: This retrospective study analyzed 150 patients who underwent serial CCTA examinations. Following strict alignment of CTA volume data with plaque masks, traditional machine learning models (LASSO, Elastic Net, Random Forest, XGBoost) and a lightweight 3D-CNN model were constructed. RPP was defined as an annualized plaque burden (PB) increase ≥ 1.0%. Model performance was primarily evaluated using the area under the receiver operating characteristic curve (AUC), with SHAP (SHapley Additive exPlanations) employed for model interpretation. *Results*: Traditional models demonstrated limited discriminatory ability, with AUCs ranging from 0.32 to 0.51. The developed 3D-CNN model achieved an AUC of 0.75 on the independent test set, with a sensitivity of 0.64 and a specificity of 0.88. SHAP analysis revealed that the 3D-CNN focused on internal plaque texture and Hounsfield Unit (HU) distribution patterns, whereas traditional models relied on limited features such as plaque volume. *Conclusion*: The 3D-CNN model can directly learn deep features associated with RPP from CCTA images. Its performance is significantly superior to traditional models and demonstrates potential comparable to current advanced radiomics and machine learning methods, offering a novel tool for non-invasive identification of high-risk plaques using a single time-point baseline scan.

Keywords: Coronary CT angiography; Plaque progression; Machine learning; Deep learning; Radiomics; Neural networks; Explainable artificial intelligence

Online publication: December 31, 2025

1. Introduction

Rapid plaque progression (RPP) is a significant predictor of acute coronary events [1,2]. Serial invasive angiographic studies have confirmed that non-obstructive lesions can progress rapidly, constituting a key mechanism for subsequent acute events [3,4]. Compared to slowly progressing plaques, RPP is significantly associated with an increased risk of future major adverse cardiovascular events [5,6]. Therefore, early identification of plaques at risk for rapid progression is crucial for preventing acute coronary syndromes. Coronary CT angiography (CCTA) is a preferred non-invasive imaging modality for evaluating coronary artery disease [7]. Recently, quantitative plaque analysis based on CCTA has emerged as a new direction for risk assessment [8]. However, traditional methods often rely on manually extracted morphological features (e.g., plaque burden, component volumes), which may inadequately capture the internal heterogeneity, microenvironment, and complex spatiotemporal dynamics of plaques [9,10].

Radiomics enables precise disease phenotyping beyond visual assessment by extracting high-dimensional quantitative features from medical images [11]. Recent studies suggest that CCTA-based radiomics aids in identifying high-risk plaques and predicting their progression [12,13]. Furthermore, machine learning (ML) frameworks can integrate clinical, laboratory, qualitative, and quantitative CCTA features to effectively identify individuals at risk of RPP [14,15]. Despite advances in radiomics and ML, these methods predominantly rely on pre-defined, handcrafted features, potentially failing to capture all spatial contextual information inherent in the raw 3D image data. Three-dimensional convolutional neural networks (3D-CNNs) can learn hierarchical feature representations end-to-end from raw image data, offering a new avenue for more fully leveraging information within CCTA images [16,17]. Based on this rationale, this study aimed to develop a lightweight 3D-CNN model for predicting RPP and to systematically compare and validate its performance against traditional ML models and advanced radiomics methods reported in the literature.

2. Materials and methods

2.1. Study population

This retrospective study was approved by the Institutional Review Board, with a waiver for informed consent. We consecutively screened patients who underwent at least two CCTA examinations at Gongli Hospital of Shanghai Pudong New Area between January 2017 and November 2024.

The inclusion criteria were as follows:

(1) An interval of ≥ 1 year between the two CCTA scans;

(2) Presence of at least one atherosclerotic plaque (diameter > 2 mm) on the baseline CCTA.

The exclusion criteria were as follows:

(1) Poor image quality precluding plaque analysis;

(2) Coronary revascularization performed between the two CCTA examinations;

(3) Missing clinical data.

A total of 150 patients were finally enrolled and randomly split into a training set (105 patients, 70%) and a test set (45 patients, 30%). Based on an annualized PB increase ≥ 1.0%, patients were categorized into a progression group (n = 64) and a non-progression group (n = 86). Baseline characteristics are shown in **Table 1**.

Table 1. Baseline patient characteristics

Variable	Overall (n = 150)	Progression group (n = 64)	Non-progression group (n = 86)	*P*-value
Demographics				
Age, years	61.2 ± 8.9	63.5 ± 8.7	59.4 ± 8.8	0.721
Male, n (%)	85 (56.7)	40 (62.5)	45 (52.3)	0.205
Body mass index, kg/m^2	25.4 ± 3.3	25.9 ± 3.5	25.0 ± 3.1	0.087
Cardiovascular risk factors, n (%)				
Hypertension	82 (54.7)	42 (65.6)	40 (46.5)	0.019
Diabetes mellitus	33 (22.0)	20 (31.3)	13 (15.1)	0.016
Dyslipidemia	56 (37.3)	26 (40.6)	30 (34.9)	0.471
Smoking history	45 (30.0)	25 (39.1)	20 (23.3)	0.132
Laboratory findings				
Total Cholesterol, mmol/L	4.70 ± 1.18	4.65 ± 1.22	4.74 ± 1.15	0.642
LDL-C, mmol/L	2.88 ± 0.87	2.92 ± 0.91	2.85 ± 0.84	0.618
HDL-C, mmol/L	1.23 ± 0.30	1.18 ± 0.28	1.27 ± 0.31	0.046
Triglycerides, mmol/L	1.66 ± 0.98	1.72 ± 1.05	1.61 ± 0.92	0.482
Morphological analysis				
Plaque length, mm	15.8 ± 8.3	18.9 ± 8.7	13.4 ± 7.2	< 0.001
Total plaque volume, mm^3	185.6 ± 128.4	258.3 ± 142.7	130.5 ± 88.6	< 0.001
Stenosis degree, %	38.7 ± 18.2	46.3 ± 18.9	32.9 ± 15.4	< 0.001
Minimal lumen area, mm^2	4.0 ± 2.2	3.2 ± 1.9	4.6 ± 2.3	< 0.001
Plaque composition analysis				
Calcified volume, mm^3	38.9 ± 47.2	52.4 ± 53.8	28.7 ± 38.5	0.002
Calcified volume ratio, %	20.9 ± 15.8	20.3 ± 15.2	21.4 ± 16.3	0.659
Non-calcified volume, mm³	146.7 ± 102.3	205.9 ± 118.6	101.8 ± 72.4	< 0.001
Non-calcified volume ratio, %	79.1 ± 15.8	79.7 ± 15.2	78.6 ± 16.3	0.659
Low-attenuation plaque volume, mm^3	9.8 ± 13.6	15.3 ± 16.8	5.6 ± 8.9	< 0.001
Low-attenuation plaque ratio, %	5.3 ± 6.8	5.9 ± 7.1	4.8 ± 6.5	0.325
Mean CT value of LAP, HU	27.8 ± 17.9	24.6 ± 15.8	30.2 ± 19.1	0.038
Fat attenuation index (FAI), HU	-69.8 ± 7.6	-67.2 ± 7.1	-71.8 ± 7.4	< 0.001
Plaque burden, %	52.3 ± 11.8	58.7 ± 10.9	47.4 ± 10.2	0.005
Annualized ΔPB, %/year	0.8 ± 2.3	2.1 ± 1.5	-0.3 ± 0.8	< 0.001
High-risk plaque features, n (%)				
Positive remodeling	92 (61.3)	48 (75.0)	44 (51.2)	0.003
Low-density plaque	28 (18.7)	18 (28.1)	10 (11.6)	0.009
Spotty calcification	25 (16.7)	14 (21.9)	11 (12.8)	0.128
Napkin-ring sign	3 (2.0)	2 (3.1)	1 (1.2)	0.381

LDL-C: Low-density lipoprotein cholesterol; HDL-C: High-density lipoprotein cholesterol; LAP: Low-attenuation plaque; HU: Hounsfield units; PB: Plaque burden; ΔPB: Change in plaque burden.

2.2. CCTA image acquisition and preprocessing

All CCTA examinations were performed using a Siemens dual-source CT scanner (Somatom Definition Flash, Siemens Healthineers, Forchheim, Germany). Image acquisition and reconstruction parameters were as follows: tube voltage 120 kVp, tube current modulated automatically based on patient body mass index (range 350–600 mA), and collimation width 64 × 0.6 mm. All original DICOM data underwent strict quality control. Prior to scanning, all patients received sublingual nitroglycerin (0.5 mg). Beta-blockers were administered for heart rate control if the pre-scan heart rate was > 65 beats per minute. Plaque quantification was performed using the United Imaging Intelligence CTA Coronary AI Analysis System (www.uii-ai.com). Plaque segmentation and annotation were conducted using ITK-SNAP (version 4.0).

Custom Python scripts (analyze_alignment.py) were used to perform slice-by-slice verification of spatial coordinates, slice thickness, and pixel spacing between the CTA volume data and corresponding plaque masks for each case. Alignment reports were generated to exclude mismatched samples.

Following previous studies, plaque volume subtypes were measured based on Hounsfield Unit (HU) thresholds: low-attenuation plaque (< 30 HU), non-calcified plaque (30–130 HU), and calcified plaque (> 130 HU). RPP was defined as an annualized plaque burden (PB) increase ≥ 1.0% [8,18]. PB was calculated as (Plaque Volume / Vessel Volume) × 100%. The annualized PB progression (ΔPB/year) was calculated as (Follow-up PB - Baseline PB) / Scan interval time (years).

2.3. Feature extraction and model construction

2.3.1. Traditional machine learning models

The model was implemented using the make_features_and_models.pyscript. A set of features was extracted from each plaque region of interest (ROI), including geometric features (volume, aspect ratio), HU statistical features (mean, standard deviation, etc.), and calcification ratio, among other radiomics features. These were merged with plaque attributes (type, stenosis degree) from clinical follow-up sheets and patient risk factors to form a structured feature table. LASSO, Elastic Net, Random Forest, and XGBoost models were constructed. Hyperparameter optimization was performed using case-stratified 5-fold cross-validation. Model performance was evaluated on the fixed independent test set.

2.3.2. 3D-CNN model

The model was implemented using the train_cnn_min.pyscript.

The input data are as follows:

(1) Image input: A 96×96×96 voxel 3D image patch was cropped from the aligned CTA volume data, centered on the plaque centroid. HU values were windowed (-100 to 500 HU) and normalized;

(2) Tabular features: 26-dimensional clinical and plaque tabular features were concatenated.

A lightweight 3D-CNN served as the backbone, incorporating Squeeze-and-Excitation (SE) attention modules to enhance feature representation. The final fully connected layers fused the imaging and tabular features to output a risk probability.

Data augmentation and regularization techniques included label smoothing (smoothing = 0.1), MixUp (α = 0.4), and CutMix (α = 0.1). The model was trained using the AdamW optimizer with cosine annealing learning rate decay, and early stopping was implemented to prevent overfitting.

2.4. Statistical analysis and model interpretation

Statistical analyses were performed using SPSS (version 26.0, IBM, Armonk, NY, USA) and R software (version 4.1.2, R Foundation, Vienna, Austria). Continuous variables were compared using the independent samples t-test or Mann-Whitney U test, as appropriate. Categorical variables are presented as frequencies and percentages, and compared using the chi-square test. The AUC, sensitivity, specificity, accuracy, and F1-score were calculated for all models. The DeLong test was used to compare differences in ROC curves. SHAP analysis was applied to the 3D-CNN model to quantify the contribution of each feature to the model predictions and identify key predictors.

3. Results

3.1. Model performance comparison

As shown in **Table 2**, the four traditional machine learning models demonstrated poor discriminatory ability on the test set (AUC range: 0.32–0.51). In contrast, the proposed 3D-CNN model achieved the best performance, with an AUC of 0.75 (95% CI: 0.69–0.81), a sensitivity of 0.64, and a specificity of 0.88.

Table 2. Performance comparison of different models on the test set

Model	AUC (95% CI)	Sensitivity	Specificity	F1-Score
LASSO	0.32 (0.25–0.39)	0.21	0.80	0.18
Elastic Net	0.35 (0.28–0.42)	0.24	0.82	0.21
Random Forest	0.48 (0.41–0.55)	0.38	0.79	0.35
XGBoost	0.51 (0.44–0.58)	0.42	0.81	0.39
3D-CNN	0.75 (0.69–0.81)	0.64	0.88	0.68

3.2. ROC curve analysis

The ROC curves for the traditional ML models were close to the diagonal, indicating limited discriminatory ability (**Figure 1**). In contrast, the ROC curve for the 3D-CNN model demonstrated superior classification performance, with an AUC of 0.75 (95% CI: 0.69–0.81) on the test set, which was significantly higher than all traditional models (DeLong test, $P < 0.01$). This result visually underscores the advantage of the 3D-CNN in identifying rapid plaque progression (**Figure 2**).

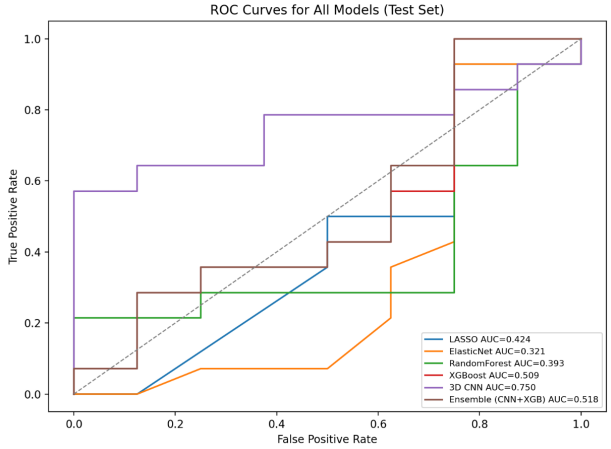

Figure 1. ROC curves for all models (test set).

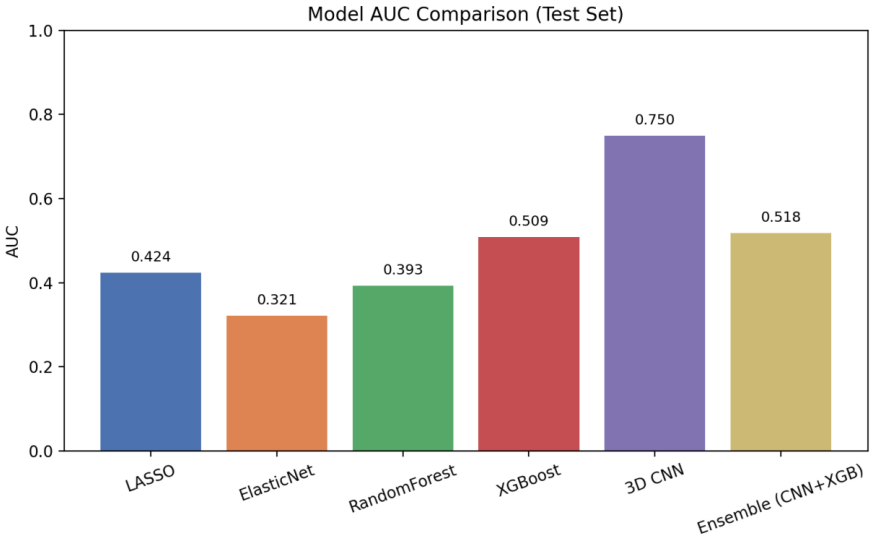

Figure 2. Model AUC comparison(test set).

3.3. Model interpretability analysis

To understand the models' decision-making basis, SHAP analysis was applied. For the best-performing traditional model (XGBoost), SHAP analysis indicated that its decisions primarily relied on traditional radiomics features such as plaque volume and the standard deviation of HU values (**Figure 3**). For the 3D-CNN model, SHAP analysis revealed that its decisions depended on a different set of feature patterns, corresponding to activations in the network's intermediate layers, which reflect local textural heterogeneity and complex HU distributions within the plaque (**Figure 4** and **Figure 5**).

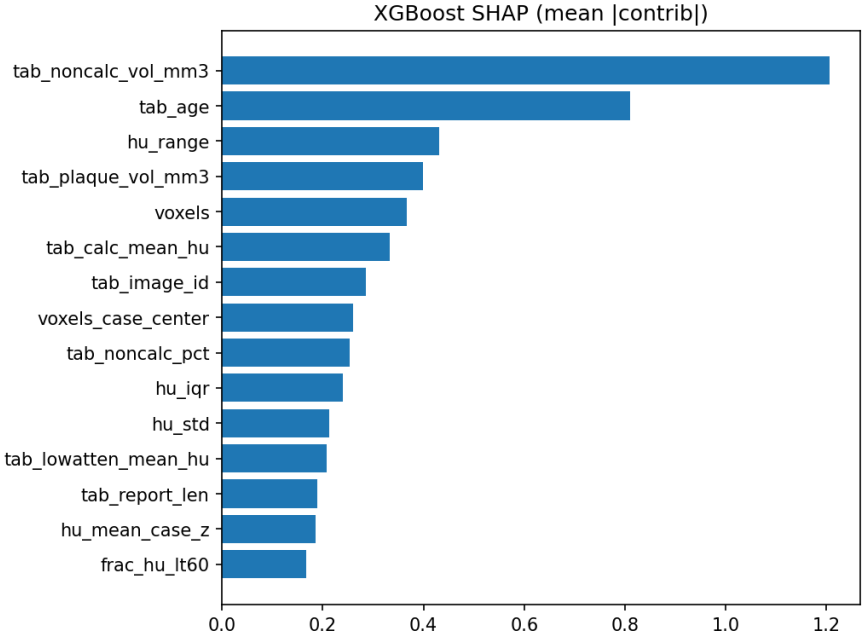

Figure 3. SHAP summary plot for the XGBoost model.

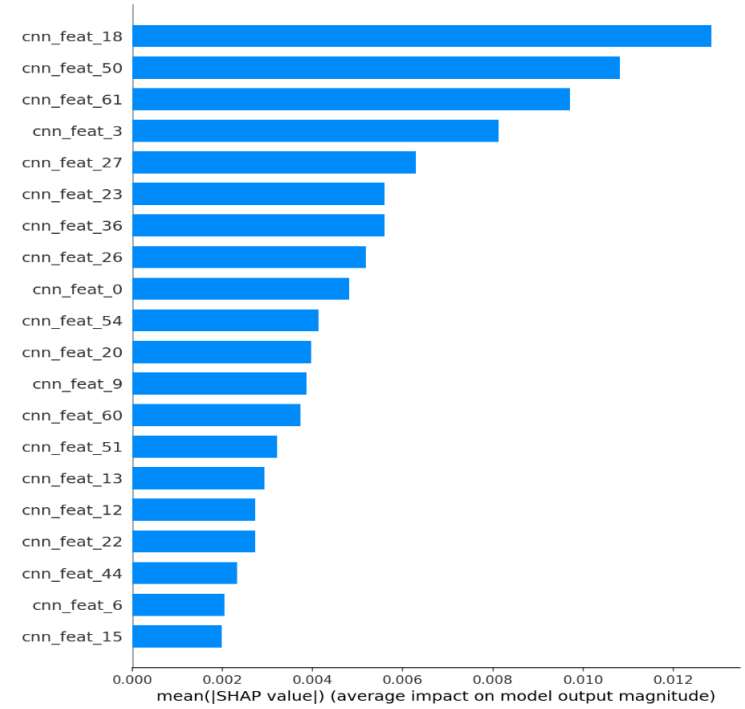

Figure 4. SHAP summary plot for the 3D-CNN model.

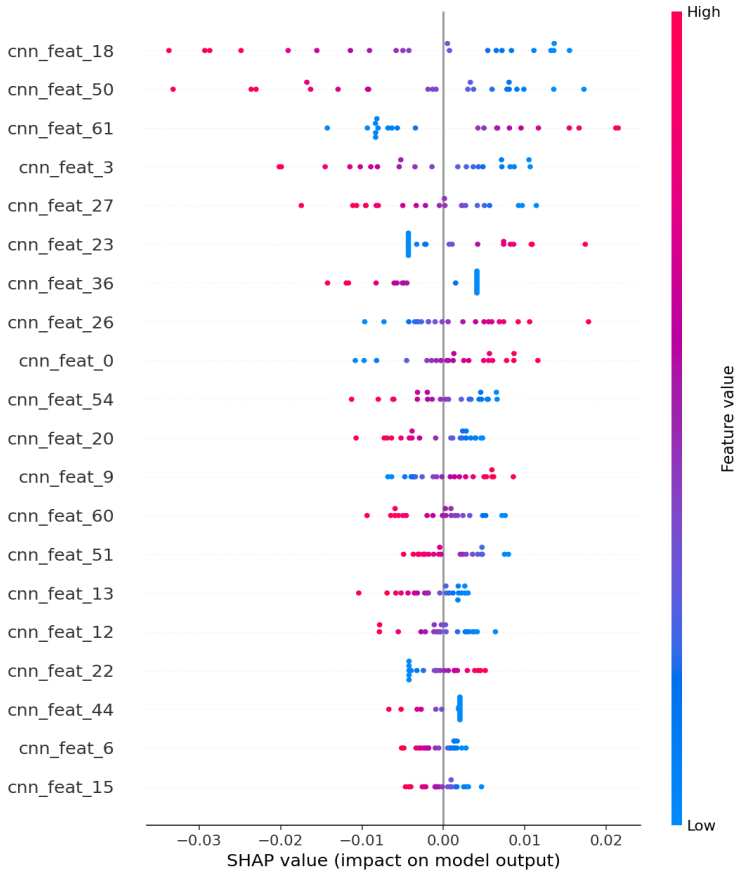

Figure 5. Representative intermediate-layer activations of the 3D-CNN model.

4. Discussion

4.1. Cross-method performance comparison and paradigm shift

The poor performance of traditional ML models (AUC: 0.32–0.51) aligns with findings by Feng *et al.*, who also reported limited performance using traditional plaque parameters, underscoring the constraints of relying solely on morphological features for predicting plaque progression [19]. In contrast, our 3D-CNN model demonstrated significantly superior performance (AUC = 0.75). This AUC is comparable to models built on radiomics signatures by Chen *et al.* (AUC 0.81–0.82) and deep learning frameworks reported by Lin *et al.*, indicating the potential of 3D-CNNs to compete with current state-of-the-art prediction tools [12,16]. SHAP analysis further elucidated the reason for this performance gap: traditional models relied on limited features like plaque volume, consistent with studies emphasizing the importance of plaque burden, whereas the 3D-CNN automatically focused on internal plaque texture and HU distribution patterns [20]. This finding resonates with radiomics studies by Chen *et al.* and Feng *et al.*, which identified features related to textural heterogeneity (e.g., wavelet-based gray-level non-uniformity) as highly predictive [13,19]. This signifies an important paradigm shift, where plaque risk assessment is evolving from a morphology-based "how big is it" approach towards a qualitative and heterogeneity-based "what does it look like inside" analysis.

4.2. Biological interpretation of features and methodological complementarity

The "texture" features emphasized by our 3D-CNN may be biologically congruent with the heterogeneity features extracted via pre-defined filters in radiomics studies. Both point towards the spatial complexity and compositional instability of plaque as the intrinsic driver of rapid progression. This aligns with the pathological mechanisms revealed by natural history studies using intravascular ultrasound (IVUS), where intra-plaque heterogeneity and microenvironmental changes are key markers of active progression [2,18]. Methodologically, this study highlights the contrast and complementarity between deep learning and radiomics. Radiomics offers good interpretability through pre-defined features, while 3D-CNNs can automatically learn more complex spatial patterns. Both approaches converge on the core concept of "image heterogeneity," providing a rationale for future hybrid models that leverage the strengths of both.

4.3. Clinical translation and precision prevention

Current ESC guidelines emphasize risk stratification and precise preventive strategies for patients with chronic coronary syndromes [7,21]. Clinical decision-making often relies on periodic CCTA re-evaluation to detect plaque progression, potentially leading to delayed intervention. The primary clinical value of our 3D-CNN model lies in its potential to identify plaques with a high-risk "trajectory" for rapid progression using only a single baseline CCTA scan, even if they appear stable at the time of imaging. This could serve as a decision-support tool, enabling intensification of lipid-lowering therapy or other targeted interventions for high-risk patients (e.g., those with hypertension, diabetes, or lower HDL-C levels, as suggested by our data) at an earlier stage. This facilitates a shift from reactive treatment to proactive prevention, aligning perfectly with evidence-based precision medicine principles [22].

4.4. Limitations and future directions

This study has several following limitations:

(1) As a single-center retrospective study, selection bias is inevitable, and the sample size, while reasonable, could be larger for a deep learning model;

(2) Although widely used, the definition of RPP based on annualized PB change requires validation against hard clinical endpoints (e.g., myocardial infarction) in long-term follow-up studies.

Future research should focus on as follows:

(1) External validation: Prospective, multi-center, large-scale validation to assess the model's generalizability and robustness;

(2) Association with clinical endpoints: Long-term follow-up to directly link model predictions to hard endpoints like acute coronary events, establishing its definitive prognostic value;

(3) Technical integration: Exploring hybrid prediction models that more deeply integrate deep learning, radiomics, and clinical risk factors;

(4) Workflow integration: Developing automated, integrated analysis pipelines incorporating image segmentation and prediction into clinical workstations to enhance practicality.

5. Conclusion

This study successfully developed a model for predicting coronary plaque progression based on a single baseline CCTA scan. The results demonstrate that a 3D convolutional neural network, incorporating concepts from radiomics, significantly outperforms traditional machine learning models. Its performance is comparable to current advanced radiomics and deep learning methods reported internationally. This confirms the substantial application potential and clinical translation value of advanced image analysis techniques for the precise risk assessment of coronary plaques.

Disclosure statement

The authors declare no conflict of interest.

References

[1] Stone G, Maehara A, Lansky A, et al., 2011, A Prospective Natural-History Study of Coronary Atherosclerosis. New England Journal of Medicine, 364(3): 226–35.

[2] Erlinge D, Maehara A, Ben-Yehuda O, et al., 2021, Identification of Vulnerable Plaques and Patients by Intracoronary Near-Infrared Spectroscopy and Ultrasound (PROSPECT II): A Prospective Natural History Study. The Lancet, 397(10278): 985–995.

[3] Yokoya K, Takatsu H, Suzuki T, et al., 1999, Process of Progression of Coronary Artery Lesions from Mild or Moderate Stenosis to Moderate or Severe Stenosis: A Study based on Four Serial Coronary Arteriograms per Year. Circulation, 100(9): 903–909.

[4] Ojio S, Takatsu H, Tanaka T, et al., 2000, Considerable Time from the Onset of Plaque Rupture and/or Thrombi until the Onset of Acute Myocardial Infarction in Humans: Coronary Angiographic Findings within 1 Week Before the Onset of Infarction. Circulation, 102(17): 2063–2069.

[5] Ahmadi A, Leipsic J, Blankstein R, et al., 2015, Do Plaques Rapidly Progress Prior to Myocardial Infarction? The Interplay between Plaque Vulnerability and Progression. Circulation Research, 117(5): 450–458.

[6] Jernberg T, Hasvold P, Henriksson M, et al., 2015, Cardiovascular Risk in Post-Myocardial Infarction Patients: Nationwide Real World Data Demonstrate the Importance of a Long-Term Perspective. European Heart Journal,

36(19): 1163–70.

[7] Knuuti J, Wijns W, Saraste A, et al., 2019, ESC Guidelines for the Diagnosis and Management of Chronic Coronary Syndromes. European Heart Journal, 41(3): 407–477.

[8] Serruys P, Hara H, Garg S, et al., 2021, Coronary Computed Tomographic Angiography for Complete Assessment of Coronary Artery Disease: JACC State-of-the-Art Review. Journal of the American College of Cardiology, 78(7): 713–736.

[9] Van Assen M, Varga-Szemes A, Schoepf U, et al., 2020, Automated Plaque Analysis for the Prognostication of Major Adverse Cardiac Events. European Journal of Radiology, 2020(116): 76–83.

[10] Lee S, Sung J, Rizvi A, et al., 2018, Quantification of Coronary Atherosclerosis in the Assessment of Coronary Artery Disease. Circulation: Cardiovascular Imaging, 11(7): e007562.

[11] Gillies R, Kinahan P, Hricak H, 2016, Radiomics: Images are More than Pictures, They are Data. Radiology, 278(2), 563–577.

[12] Chen Q, Xie G, Tang C, et al., 2023, Development and Validation of CCTA-based Radiomics Signature for Predicting Coronary Plaques With Rapid Progression. Circulation: Cardiovascular Imaging, 16(2): e014711.

[13] Chen Q, Pan T, Wang Y, et al., 2023, A Coronary CT Angiography Radiomics Model to Identify Vulnerable Plaque and Predict Cardiovascular Events. Radiology, 307(2): e221693.

[14] Han D, Kolli K, Al'Aref S, et al., 2020, Machine Learning Framework to Identify Individuals at Risk of Rapid Progression of Coronary Atherosclerosis: From the PARADIGM Registry. Journal of the American Heart Association, 9(5): e013958.

[15] Motwani M, Dey D, Berman D, et al., 2017, Machine Learning for Prediction of All-Cause Mortality in Patients with Suspected Coronary Artery Disease: A 5-year Multicentre Prospective Registry Analysis. European Heart Journal, 38(6): 500–507.

[16] Lin A, Manral N, McElhinney P, et al., 2022, Deep Learning-Enabled Coronary CT Angiography for Plaque and Stenosis Quantification and Cardiac Risk Prediction: An International Multicentre Study. The Lancet Digital Health, 4(4): e256–e265.

[17] Sehly A, He A, Jaltotage B, et al., 2024, Coronary Artery Stenosis and Vulnerable Plaque Quantification on CCTA by Deep Learning Methods. European Heart Journal, 43(Supplement_1): ehad655.187.

[18] Nicholls S, Hsu A, Wolski K, et al., 2010, Intravascular Ultrasound-Derived Measures of Coronary Atherosclerotic Plaque Burden and Clinical Outcome. Journal of the American College of Cardiology, 55(21): 2399–2407.

[19] Feng C, Chen R, Dong S, et al., 2023, Predicting Coronary Plaque Progression with Conventional Plaque Parameters and Radiomics Features Derived from Coronary CT Angiography. European Radiology, 33(5): 3132–3143.

[20] Mortensen M, Dzaye O, Steffensen F, et al., 2020, Impact of Plaque Burden Versus Stenosis on Ischemic Events in Patients With Coronary Atherosclerosis. Journal of the American College of Cardiology, 76(19): 2213–2222.

[21] Byrne R, Rossello X, Coughlan J, et al., 2023, ESC Guidelines for the Management of Acute Coronary Syndromes. European Heart Journal, 44(38): 3720–3826.

[22] Williams M, Kwiecinski J, Doris M, et al., 2020, Low-Attenuation Noncalcified Plaque on Coronary Computed Tomography Angiography Predicts Myocardial Infarction: Results From the Multicenter SCOT-HEART Trial (Scottish Computed Tomography of the HEART). Circulation, 141(18): 1452–1462.